INSTITUTE OF PHYSICS PUBLISHING JOURNAL OF PHYSICS B: ATOMIC, MOLECULAR AND OPTICAL PHYSICS

J. Phys. B: At. Mol. Opt. Phys. **39** (2006) 1899–1912 doi:10.1088/0953-4075/39/8/008

Photodouble ionization studies of the Ne($2s^2$) state under unequal energy sharing conditions

P Bolognesi[1], A Kheifets[2], S Otranto[3,7], M Coreno[1,4], V Feyer[1,5], F D Colavecchia[6], C R Garibotti[6] and L Avaldi[1,4]

[1] CNR-IMIP, Area della Ricerca di Roma 1, Monterotondo Scalo, Rome, Italy
[2] Research School of Physical Sciences and Engineering, Australian National University, Canberra, Australia
[3] Physics Department, University of Missouri-Rolla, Rolla MO, USA
[4] CNR-TASC, Gas Phase Photoemission Beamline at Elettra, Area Science Park, Trieste, Italy
[5] Institute of Electron Physics, National Academy of Sciences, Uzhgorod, Ukraine
[6] CONICET and Centro Atómico Bariloche, 8400 SC de Bariloche, Argentina
[7] CONICET and Depto. de Física, Universidad Nacional del Sur, 8000 Bahía Blanca, Argentina

Received 1 December 2005, in final form 22 February 2006
Published 3 April 2006
Online at stacks.iop.org/JPhysB/39/1899

Abstract

The triple differential cross section (TDCS) of the $He^{2+}(1s^{-2})$ and $Ne^{2+}(2s^{-2})$ states has been studied under unequal energy sharing conditions and perpendicular geometry, for a ratio of about 3 between the energies of the two ejected electrons. The dynamical quantities which govern the photodouble ionization (PDI) process, i.e. the squared moduli of the gerade and ungerade complex amplitudes and the cosine of their relative phase, have been extracted from the experimental data. The results from the two targets have been compared between themselves as well as with the theoretical predictions of the SC3 and convergent close coupling (CCC) calculations. This work represents a joint experimental and theoretical approach to the investigation of PDI of atomic systems with more than two electrons.

1. Introduction

Since the first pioneering experiment of Schwarzkopf *et al* [1], the photodouble ionization (PDI) studies of He have been rapidly shown to be a powerful tool for the understanding of the few-body Coulomb problem, a fundamental process in atomic physics. Indeed, the PDI of the He atom, with the simple $^1P^o$ symmetry of the electron pair and just a bare nucleus with no internal structure in the final state, is the prototypical example of the three-body Coulomb problem and the most suited process to study the electron–electron correlations. From the experimental point of view, the complete characterization of the PDI implies the measurement of the triple differential cross section (TDCS), $d^3\sigma/d\Omega_1\, d\Omega_2\, dE_1$, where

either both the photoelectrons [1] or a photoelectron and the residual ion [2] are detected in coincidence with energy (E_i) and angular ($\Omega_i = (\theta_i, \varphi_i)$ with $i = 1, 2$) selectivity.

In about 10 years time, a large amount of data has been obtained for He [3] and theoretical models, based on both computational and analytical approaches, have been developed [3, 4]. A fairly good agreement among theories and between theory and experiments has been reached providing a reasonably good understanding of this process. Moreover, considering that the TDCS at a fixed excess energy can be measured under a large variety of kinematics conditions, methods [5, 6] of extracting the basic quantities, namely the moduli and related phases of the gerade and ungerade complex amplitudes of the process from the experimental data, have been proposed. These were shown to be a very useful tool for a comparison between theory and experiments.

It has already been few years since the experiments on PDI have begun to consider targets other than He. In most cases, the outer np shell of the rare gases heavier than He has been studied ([7] and references therein). These experiments offer the opportunity to test our understanding of the PDI process in cases where different initial and final states are involved as well as when the indirect mechanisms, that take place when double ionization proceeds via the excitation and decay of an intermediate state of the singly charged ion, may occur. However, the complexity of the description of many-electron atoms has so far hampered a full extension of the theoretical models developed for He [8–10]. The use of parameterization formulae, such as the 'partial wave model' [11] or a more general '*exact*' formula based on the expansion of the correlated final state wavefunction on the basis of bipolar harmonics [12] has also been proposed. However, even though providing a good representation of the data, both approaches have shown their limitations in the interpretation of the fitting parameters [7, 13].

The PDI of Ne(2s) has the advantage of being a He-like system as far as the final state symmetries are concerned. Indeed, the symmetries of both the residual ion and the electron pair, $^1S^e$ and $^1P^o$, respectively, are the same in the two gases, simplifying the theoretical description. Thus, a joint theoretical and experimental effort [14, 15] has been undertaken recently to study the PDI under equal energy sharing condition, at about 20 eV above the double ionization threshold. Despite the similarities to the He case, the Ne experimental results showed that the TDCS is significantly different from the equivalent He case, measured at the same excess energy above the double ionization threshold. These differences consisted in narrower and tilted lobes and in the appearance of extra features, particularly evident in the forward direction when the fixed electron was detected at 0° with respect to the light polarization axis. These features have been attributed to an initial state effect. Indeed, agreement between experiment and theories [14, 15] has been achieved only via a proper description of the initial state wavefunction which takes into account the intrashell correlation among the Ne 2p and 2s shells.

After this first successful step in the investigation of the PDI of Ne(2s), we have now considered a more challenging situation of unequal energy sharing between the two ejected electrons, where both the gerade and ungerade amplitudes as well as their relative phase contribute to determining the TDCS.

In this work, we present the TDCS of the He(1s) and Ne(2s) states measured at about 22 eV excess energy, in perpendicular geometry and under unequal energy sharing condition, $E_1 = 6$ eV and $E_2 = 16.5$ eV, i.e. a ratio of about 3 between the energies of the two ejected electrons. For each gas, the experimental results consist of three internormalized TDCSs measured at $\theta_1 = 0°$, 30° and 60° relative to the polarization axis of light. Then, applying the method recently proposed by Bolognesi *et al* [5] we have extracted the basic dynamical parameters of the TDCS. These have been compared with the predictions of the convergent

close coupling (CCC) [16] and SC3 [17] calculations emphasizing similarities and differences between the two cases.

The paper is organized as follows: details of the experimental setup are reported in section 2 while some general information about the SC3 and CCC theoretical models are contained in section 4; the procedures of data analysis, the results and the comparison with the theoretical calculations are discussed in section 4 and some conclusions are finally made in the last section.

2. Experimental details

The experiments have been performed using the multi-coincidence endstation [18] of the gas phase photoemission beamline [19] of the Elettra storage ring in Trieste, Italy. The light source is an undulator of period 12.5 cm, 4.5 m long. The linearly polarized radiation from the undulator is deflected to the variable-angle-spherical grating monochromator [20] by a prefocusing mirror. The monochromator consists of two optical elements: a plane mirror and a spherical grating. Five interchangeable gratings cover the energy region of 13–1000 eV. Two refocusing mirrors after the exit slits provide a circular focus (radius of about 300 μm) at the interaction region in the experimental chamber.

The endstation [18] is equipped with ten independent electrostatic analysers, arranged in two groups of three and seven analysers respectively, mounted on two separate turntables. The three analysers of the small turntable are placed at 0°, 30° and 60° with respect to the polarization axis of the photon beam and they have been used to detect the electrons, of kinetic energy $E_1 = 6$ eV, at fixed directions with respect to the polarization of the incident radiation. The seven analysers mounted on the bigger turntable are all placed at 30° from each other. By successive rotations of this turntable, they are used to measure the angular distribution of the correlated photoelectron of complementary energy $E_2 = h\nu - IP^{2+} - E_1$, where IP^{2+} is the ionization potential of the doubly charged ion state under investigation and $h\nu$ is the incident photon energy. For the present experiments, both frames have been kept in the plane perpendicular to the direction of the incoming photon beam, z. For both the He and Ne cases, the energy of the second photoelectron was $E_2 = 16.5$ eV, corresponding to the incident photon energies of 101.5 and 144.4 eV, for He and Ne, respectively. The energy resolution and the angular acceptance in the dispersion plane of the spectrometers were $\Delta E_i = 50$ and 150 meV for $i = 1$ and 2, respectively, and $\Delta\vartheta_{1,2} = \pm 3°$. Photoelectron spectra measured in Ne at few photon energies below and above the $Ne^{2+}(2s^{-2})$ double ionization threshold and around the kinetic energies, $E_{1,2}$, of interest have confirmed that no resonant process contributes to the double ionization of Ne in the chosen energy condition. This has been done because it is well known that resonance processes resulting in indirect PDI alter both the shape and the intensity of the features of the TDCS [21].

The coincidence electronics is made by three independent time-to-digital, TDC, converters. In the experiment, each TDC unit is operated in the common start mode with the signals of each one of the three analysers of the small turntable used as starts and the signals from the other seven as stops. In this way, 21 coincidence pairs are collected simultaneously. All the experimental settings and the data acquisition are controlled via a PC equipped with LabView software. The same software monitors the stability of the experiment during the long coincidence measurements via the acquisition of the non-coincidence count rates of the ten analysers and the photon flux at fixed time intervals [22].

The relative efficiency of the spectrometers has been calibrated via the measurement of the photoelectron angular distribution of He^{+*} ($n = 2$) at 6 and 16.5 eV above its threshold. At these energies, the asymmetry parameter of the angular distribution of the photoelectron is

known [23]. Then, the obtained efficiencies have been confirmed by measuring the photoelectron angular distribution of $He^+(1s^{-1})$ at the same kinetic energies. The same efficiency correction has been assumed for the coincidence measurements. The validity of this assumption has been tested by measuring the coincidence yield at two positions of the larger turntable which allow us to overlap two nearby analysers, i.e. with a rotation of the large turntable of 30°. Therefore, all the experimental data are internormalized and can be reported on a common scale of counts [22]. Under the typical experimental conditions of about 1×10^{-5} mbar of gas pressure and 6×10^{12} photon s^{-1}, acquisition times of about 3 and 10 h/point were needed in the He and Ne experiments, respectively, in order to achieve the present accuracy in the TDCS measurements.

The linear polarization of the photon beam, S_1, was verified to be equal to 1, within experimental uncertainty, at all photon energies of interest.

3. The theoretical models

The CCC method [16] is a fully numerical approach that relies on heavy computations. For the final state, it solves the Schrödinger equation for the system of a photoelectron scattering on a singly charged ion by employing the close coupling expansion of the total two-electron wavefunction. In the CCC method, the PDI results from the electron impact ionization of the singly charged He^+ ion. In He, the initial state is represented by a highly correlated Hylleraas-type wavefunction, the use of which ensures that the results have insignificant dependence on the gauge of the electromagnetic interaction. The He CCC integrated PDI cross sections and TDCS agree with the experimental ones over a broad energy range. In order to calculate the $Ne^{2+}(2s^{-2}\ 2p^6)$ TDCS, a He-like final state has been adopted in which the two photoelectrons depart in the field of the positive charge $Z = 2$. As to the initial state, a multi-configuration ground state $C_{2s}2s^2 + C_{2p}2p^2$ wavefunction, built on the basis of Hartree–Fock orbitals, has been adopted in order to incorporate the intershell correlations. The values of the C_{2s} and C_{2p} coefficients have been taken from our previous work under equal energy sharing conditions [14]. In Ne, the basis set used in the present calculations had to be increased noticeably (from 15-ℓ to 60-ℓ target eigen- and pseudostates in each partial wave from $\ell = 0$ to $\ell = 5$) with respect to the one used in the equal energy share case [14] in order to achieve stable and convergent results. The poor convergence affects particularly strongly the TDCS at zero or small fixed angle. When applied to neon, the CCC method gives close results, both in shape and in magnitude, in the length and velocity gauges. The acceleration gauge cannot be applied directly to many-shell target atom as it requires an accurate ground state wavefunction near the origin where the core electrons should be taken into account.

The SC3 is a modified version of the C3 model introduced by Garibotti and Miraglia [24] and then applied to PDI by Maulbetsch and Briggs [25]. The C3 model is an analytical model with the property to treat on equal footing the electron–ion and electron–electron interactions in the final state. SC3 considers an effective interelectronic distance through an energy-dependent boost parameter to simulate the nuclear kinematical effects in the e–e interaction and to improve the C3 behaviour in the low-energy limit. The TDCS evaluated with the SC3 model in the velocity and length gauges shows similar shapes for He(1s) target, even below 20 eV above threshold [15]. Moreover, the SC3 velocity gauge prediction leads to results closer to the experiment and in better agreement than the standard C3 model [17]. However, the magnitudes obtained in both gauges exhibit large differences mirroring the fact that different approximated Hamiltonians are used in both initial and final states.

The final state wavefunction in the two-active electrons approximation is given by

$$\Psi_f^- = e^{i\mathbf{k}_1\cdot\mathbf{r}_1+i\mathbf{k}_2\cdot\mathbf{r}_2}\,{}_1F_1[ia_1, 1, -i(k_1r_1 + \mathbf{k}_1\cdot\mathbf{r}_1)]\,x\,{}_1F_1[ia_2, 1, -i(k_2r_2 + \mathbf{k}_2\cdot\mathbf{r}_2)] \times x\,{}_1F_1[ia_{12}, 1, -i\beta(k_{12}r_{12} + \mathbf{k}_{12}\cdot\mathbf{r}_{12})], \quad (1)$$

where $k_{1;2}$ are the electrons relative momenta, a_j are the Sommerfeld parameters that relate the intensity of the interaction for a given pair of particles to their relative velocity and β is the boosting parameter. In the present case, the two 2s electrons are emitted with unequal energies. According to Belkic's prescription [26], since the slow electron is more sensitive to this charge, we approximate $Z_{\text{slow}} = 3.93$ which corresponds to the single electron removal from the 2s level of Ne [27–29]. While the slow electron feels this screened charge, the fast emitted electron follows a trajectory mainly governed by the asymptotic charge $Z_{\text{fast}} = 2$. The booster parameter β in the present approximation modifies the e–e interaction and since it should contain information on the whole system we used $\beta = Z_{\text{slow}}/2E_{\text{exc}}^{0.5}$, where $E_{\text{exc}} = E_1 + E_2$ is the excess energy of the double ionization process.

As for the initial state in Ne, two possible options have been considered: (a) the simple product of one-electron Hartree–Fock wavefunction given by Koga *et al* [30] for the Ne($2s^2$) state and (b) the multi-configuration Hartree–Fock (MCHF) approach recently proposed by Bolognesi *et al* [15], given by the combination C_{2s} ($2s^2$) + C_{2p} ($2p^2$), where C_{2s} and C_{2p} are the values indicated above and the 2s and 2p states are given in [32]. The main difference between these two approaches is that the former neglects the electron–electron angular correlation in the initial state while the latter introduces this correlation albeit through an ad hoc procedure.

4. Results

The TDCS measured at 22.5 eV excess energy, $E_1 = 6$ eV and three directions ($\theta_1 = 0^\circ$, 30° and 60°) of the fixed photoelectron with respect to the polarization axis of the photon beam are reported in figures 1 and 2 for the He and Ne cases, respectively. Two previous measurements on He have been reported in the literature at a close excess energy (20 eV) and similar $R = E_2/E_1$ [31, 32]. Generally, a good agreement is observed between the different sets of experimental data as far as the number and the position of the features in the TDCS are concerned. Small differences as for the relative intensity of the lobes and the ratios of the maxima and minima can be attributed to the different angular and energy acceptances of the data collected with various imaging techniques as well as to the different amounts of linear polarization of the incident radiation.

In figures 1 and 2, the experimental data are also compared with the predictions of the CCC and SC3 calculations. In these plots, the experimental data and the theoretical curves are internormalized, i.e. reported on a common scale of counts. Indeed, each set of theoretical calculations has been rescaled to the experimental data by one single scaling factor, as reported in table 1. In the Ne case, the results for both the (a) simple product of one-electron Hartree–Fock wavefunction and (b) MCHF calculations of the SC3 model (see section 3) have been reported. For shortness, in the following these two different approaches of the SC3 method will be labelled as SC3-S and SC3-MC, respectively. The differences in the scaling factors are linked to the absolute value of the TDCS predicted by the models (see table 1). The measurements in He at 20 eV above threshold by Bräuning *et al* [31] in a kinematic very close to the present one were reported on absolute value. CCC predictions were in very good agreement with those measurements.

For the He case (figure 1), both the SC3 and CCC theories show a very good qualitative agreement, as for the number and the position of the lobes. However, while the CCC theory also displays a quantitative agreement concerning the width and relative intensity of these

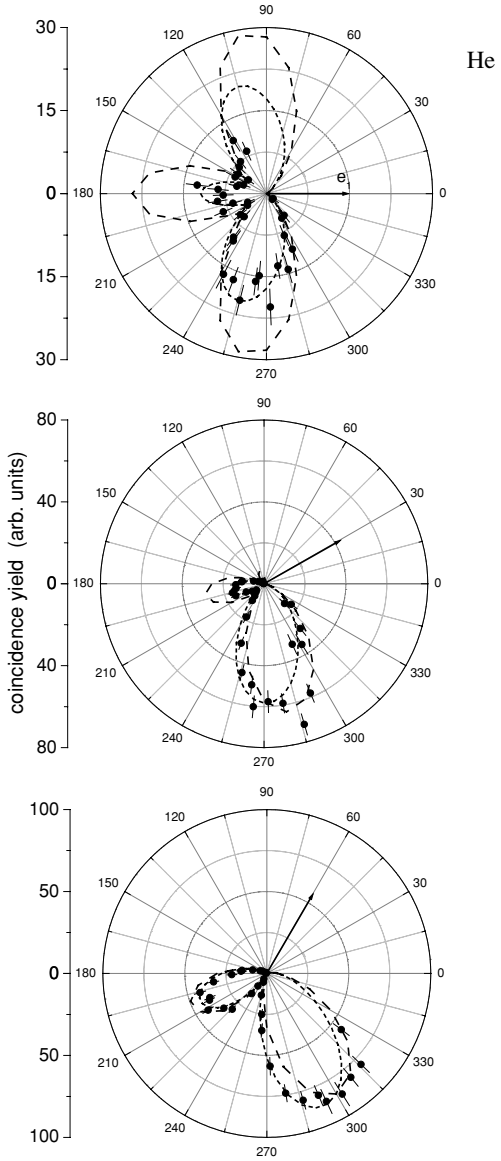

Figure 1. The $He^{2+}(1s^{-2})$ TDCS measured in perpendicular geometry, at an excess energy of 22.5 eV and the fixed electron of 6 eV. The experimental data are internormalized and compared with the predictions of the CCC (short dash line) and SC3 (dash line) models.

Table 1. Scaling factor for the CCC, SC3-S and SC3-MC calculations (see the text) and the absolute TDCS in atomic units at $\theta_1 = 60^\circ$ and $\theta_2 = 290^\circ$.

	Scaling factor He	TDCS (au) He	Scaling factor Ne	TDCS (au) Ne
SC3-S	3×10^6	2.5×10^{-5}	2.5×10^6	3.9×10^{-5}
SC3-MC	–	–	2.2×10^6	4.4×10^{-5}
CCC	0.25×10^6	3.4×10^{-5}	0.05×10^6	26.3×10^{-5}

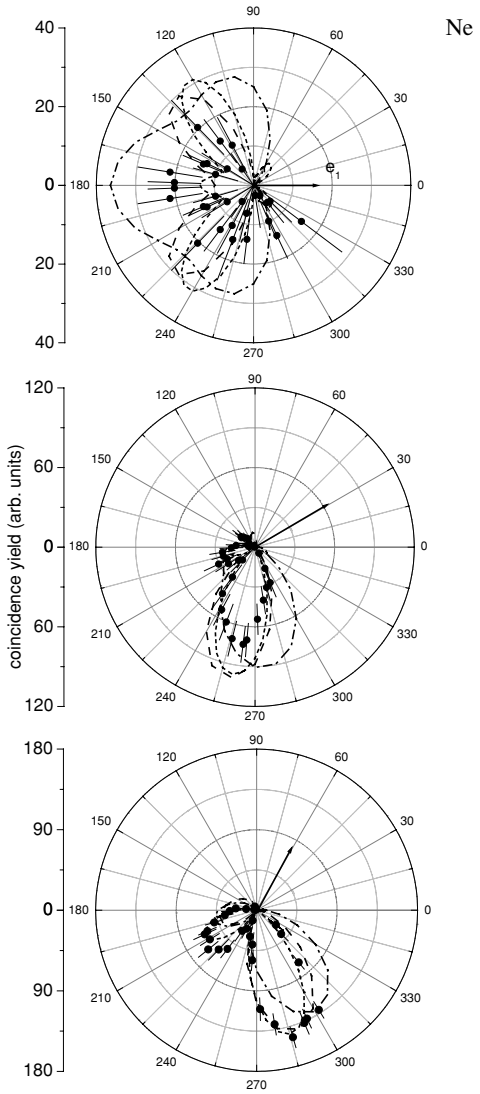

Figure 2. The $Ne^{2+}(2s^{-2})$ TDCS measured in perpendicular geometry, at an excess energy of 22.5 eV and the fixed electron of 6 eV. The experimental data are internormalized and compared with the predictions of the CCC (short dash line), SC3 model using two different initial state wavefunctions, a simple product of one-electron Hartree–Fock wavefunction (dash-dot line) and a multi-configuration Hartree–Fock approach (dash line), see the text.

lobes, the SC3 model loses its quantitative agreement as θ_1 approaches 0°, where the shape of the TDCS appears to be correct, but its relative intensity compared to the other two geometries is overestimated.

As expected, the Ne case (figure 2) is a more stringent test, especially in the condition $\theta_1 = 0^\circ$, where both the SC3-MC and CCC calculations fail to reproduce the most prominent experimental feature, i.e. a broad lobe in the backward direction. Both calculations show instead two main lobes located at about $180^\circ \pm 60^\circ$ and two smaller lobes at about 50° and

310°. Small differences can be observed in the predictions of the two models. Indeed in the CCC predictions the development of a feature in the backward direction can be observed and the small lobe at about 310° has an intensity closer to the experimental observations. The agreement among these two calculations and the experimental results improves as θ_1 is increased to 30° and then to 60°. As for the SC3-S calculation, the shape of the TDCS predicted at $\theta_1 = 0°$ is consistent with the experimental observation in the backward direction. However, the relative intensity of the TDCS with respect to those in the other measured kinematics is overestimated. At $\theta_1 = 30°$ and 60°, the position and the width of the lobes are not well reproduced by SC3-S.

Given the $^1P^o$ symmetry of the electron pair continuum wavefunction in the case of the PDI of the He($1s^2$) and Ne($2s^2$) states, the TDCS can be written in a way that allows the full separation of the geometrical factors and the dynamic parameters [33]. In the case of incident radiation that propagates along the z axis and is fully linearly polarized along the x axis, the TDCS measured in the perpendicular, (x, y), plane can be written as

$$\mathrm{TDCS}(E_1, E_2, \theta_{12}) \propto |a_g(E_1, E_2, \theta_{12})(\cos\theta_1 + \cos\theta_2) + a_u(E_1, E_2, \theta_{12})(\cos\theta_1 - \cos\theta_2)|^2, \tag{2}$$

where θ_{12} is the relative angle between the directions of emission of the two photoelectrons. The complex amplitudes a_g and a_u are respectively symmetric (gerade) and antisymmetric (ungerade) with respect to the exchange of the two electrons. Their dependence on the photoelectron energies and the relative angle contains all the dynamical information about the PDI process. However, in the TDCS this most important information can be sometimes masked by the contribution of the geometrical terms. Recently, Bolognesi *et al* [5] proposed a procedure that using a set of three relative internormalized experimental determinations of the TDCS at the same E_1, E_2 and θ_{12} values allows us to extract the square modulus of the complex amplitudes $|a_g|^2$, $|a_u|^2$ and the cosine function of their relative phase δ. This approach does not rely upon any assumption on the functional dependence of the a_g and a_u amplitudes in E_1, E_2 and θ_{12}. It has the advantage to make the comparison between experimental and theoretical results more direct and general, because it is independent upon any particular geometrical condition. Furthermore, it is a very stringent test of self-consistency for both the experimental data and the theoretical calculations. Indeed, the extracted $|a_g|^2$ and $|a_u|^2$ functions retain their dependency on θ_{12} but are independent of the particular θ_1 and θ_2 and are expected to be symmetric around $\theta_{12} = 180°$. It follows that any departure from this simple property can certainly be addressed as an inconsistency of the input data for the system [5], either theoretical or experimental. Possible sources of 'inconsistency' can be identified, for example, in the incorrect internormalization of the TDCS distributions at the three different θ_1 conditions, or a wrong relative intensity of the different features in a single TDCS distribution.

In view of these many advantages and for the more concise and general format of the results, we favoured this procedure [5] for a quantitative data analysis of the present study. $|a_g|^2$, $|a_u|^2$ and $\cos\delta$ are reported in figures 3 and 4 for the He and Ne cases, respectively. For the experimental results of figures 1 and 2, the $|a_g|^2$ and $|a_u|^2$ data that originally corresponded to a $\theta'_{12} > 180°$ have been displayed in the range $\theta_{12} < 180°$ by the shift $\theta_{12} = 360° - \theta'_{12}$.

Both the theoretical and experimental results have been fitted in their $|a_{g,u}|^2$ form, using the Gaussian approximation:

$$|a_{g,u}(E_1, E_2, \theta_{12})|^2 \propto A_{g,u} \cdot \exp\left[-4 \cdot \ln 2 \cdot \left(\frac{180 - \theta_{12}}{\Gamma_{g,u}}\right)^2\right], \tag{3}$$

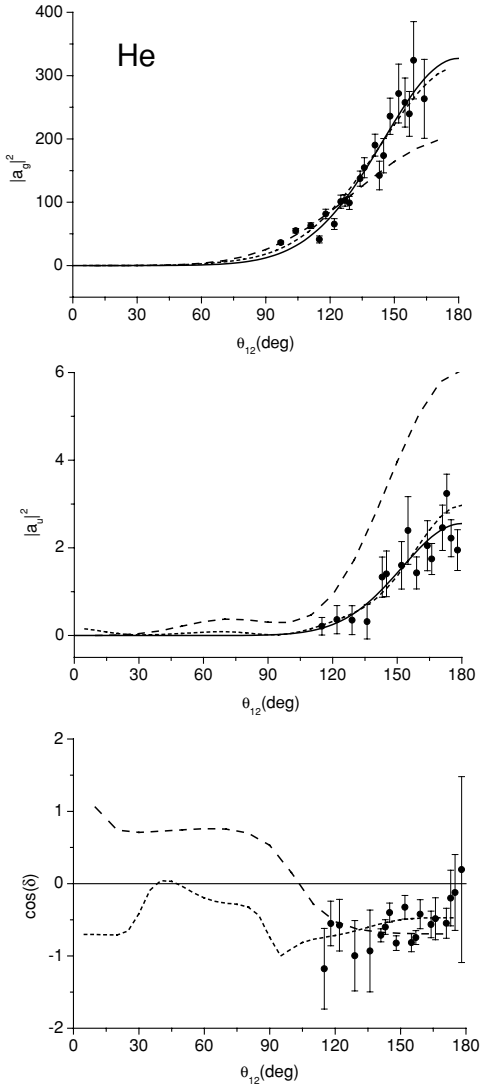

Figure 3. The dynamical parameters of the He^{2+} ($1s^{-2}$) TDCS process at $E_1 = 6$ eV and $E_2 = 16.5$ eV, as extracted [5] from the TDCS of figure 1. The experimental $|a_g|^2$, $|a_u|^2$, cos δ and their best fit (full line) are compared with the theoretical predictions of the CCC (short dash line) and SC3 (dash line) calculations.

where $A_{g,u}$ is the amplitude and $\Gamma_{g,u}$ is the full width at half maximum (FWHM) of the distribution. The accuracy of the Gaussian approximation for the gerade and ungerade amplitudes of the TDCS has been verified theoretically up to an excess energy of 60 eV [34]. So we adopted this approximation to represent the main feature of $a_{g,u}$, which is in the range of $130^\circ < \theta_{12} < 180^\circ$. This appears to be a reasonable assumption at least at the level of accuracy of the present data. However, some extra features appear at $\theta_{12} < 120^\circ$ in the theoretical predictions of the ungerade amplitudes, both for the He and Ne cases. In the latter case, the intensity of the extra feature is quite noticeable. This finding is at least qualitatively supported by the experimental results in the Ne case, where the θ_{12} range is large enough to

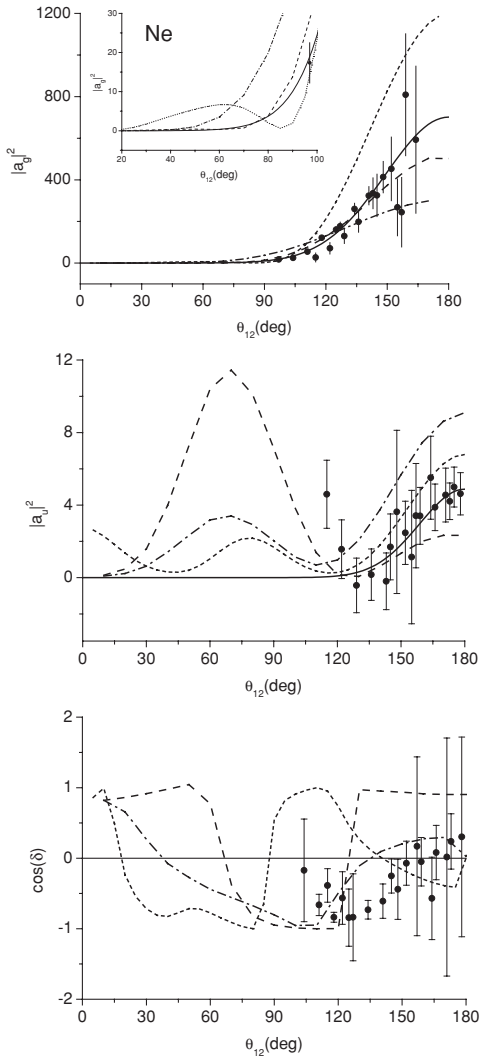

Figure 4. The dynamical parameters of the Ne^{2+} ($2s^{-2}$) TDCS process at $E_1 = 6$ and $E_2 = 16.5$ eV, as extracted [5] from the TDCS of figure 2. The experimental $|a_g|^2$, $|a_u|^2$, cos δ (dots) and their best fit (full line) are compared with the theoretical predictions of the CCC (short dash line) and SC3-S (dash-dot line) and SC3-MC (dash line) calculations.

show a rise at $\theta_{12} < 130^\circ$. However, the limited number of experimental points in that region prevents any definite statement on the real intensity of this feature. The parameters obtained by the Gaussian approximation are reported in table 2. It should be noted that the experiments do not provide absolute cross sections, so that the meaningful information is the A_g/A_u ratio, also reported in table 2. The experimental value of cos δ reported in the table is an average of the obtained values. Some information about the secondary peaks of the $|a_u|^2$ function is also reported in the same table.

The use of a constant value for cos δ was proposed by Cvejanovic and Reddish [35] in their *practical parameterization* of the PDI. In the present case, it appears to be a good

Table 2. The experimental and theoretical parameters describing the He and Ne $|a_{g,u}|^2$ and cos δ in the approximation of a Gaussian distribution for the gerade and ungerade amplitudes, the averaged phase δ. For the Ne case, the A_u and Γ_u labelled as (1) are the results of a fitting procedure and refer to the angular range $130^\circ < \theta_{12} < 180^\circ$. The ones labelled as (2) and (3) are only estimates, as read directly from the plots, of the secondary peaks appearing in $|a_{g,u}|^2$, as they could not always be represented by Gaussian functions.

	Parameter	Present experimental data	CCC	SC3	
He	Γ_g	$82.5^\circ \pm 3.7^\circ$	$87.4^\circ \pm 0.2^\circ$	$105.3^\circ \pm 0.6^\circ$	
	A_g	327.3 ± 16.1	311.2 ± 0.65	204 ± 1.1	
	Γ_u	$68.9^\circ \pm 7.8^\circ$	$60.5^\circ \pm 1.1^\circ$	$74.5^\circ \pm 0.6^\circ$	
	A_u	2.45 ± 0.18	2.88 ± 0.04	6.1 ± 0.6	
	A_g/A_u	133.6 ± 11.8	108.0 ± 1.5	33.4 ± 3.3	
	cos δ	-0.61 ± 0.07	–	–	
	$\Gamma_u(2)$	–	$\approx 33^\circ$	$\approx 50^\circ$	
	$A_u(2)$	–	≈ 0.09	≈ 0.37	
	$\theta_{12}(2)$	–	$\approx 68^\circ$	$\approx 70^\circ$	
	$\Gamma_u(3)$	–	$\leqslant 32^\circ$	–	
	$A_u(3)$	–	$\geqslant 0.15$	–	
	$\theta_{12}(2)$	–	0°	–	
Ne		Present experimental data	CCC	SC3-S	SC3-MC
	Γ_g	$72.7^\circ \pm 1.8^\circ$	$76.8^\circ \pm 0.7^\circ$	$105.3^\circ \pm 0.9^\circ$	$83.4^\circ \pm 0.5^\circ$
	A_g	702 ± 61	1226.3 ± 10.1	310.8 ± 2.5	529.5 ± 3.2
	$\Gamma_u(1)$	$50.2^\circ \pm 11.6^\circ$	$57.6^\circ \pm 0.43^\circ$	$69.7^\circ \pm 1.0^\circ$	$56.99^\circ \pm 3.19^\circ$
	$A_u(1)$	5.62 ± 1.1	6.85 ± 0.04	9.2 ± 0.1	2.61 ± 0.12
	A_g/A_u	124.9 ± 26.7	179.0 ± 1.8	33.8 ± 0.5	202.9 ± 9.4
	cos δ	-0.33 ± 0.08	–	–	–
	$\Gamma_u(2)$	$\geqslant 10^\circ$	$\approx 37^\circ$	$\approx 50^\circ$	$\approx 50^\circ$
	$A_u(2)$	$\geqslant 4.6$	≈ 0.09	≈ 3.4	≈ 11.45
	$\theta_{12}(2)$	$\leqslant 115^\circ$	$\approx 69^\circ$	$\approx 70^\circ$	$\approx 70^\circ$
	$\Gamma_u(3)$	–	$\approx 33^\circ$	–	–
	$A_u(3)$	–	≈ 2.2	–	–
	$\theta_{12}(2)$	–	$\approx 78^\circ$	–	–

approximation, at least in the region investigated experimentally for He, but not for Ne where, despite the large error bars, the values of cos δ display a definite trend.

5. Discussion

As already observed for the equal energy sharing studies [15], qualitative differences between the TDCSs of $He^{2+}(1s^{-2})$ and $Ne^{2+}(2s^{-2})$ can be observed. The first one is the appearance of 'extra' lobes at smaller angles of the Ne TDCS measured at $\theta_1 = 0^\circ$ (compare the top panels of figures 1 and 2). A similar feature was observed also in the experiment in equal energy sharing [14]. In analogy with the TDCS of the $Ne^{2+}(2p^{-2}\ {}^1S^e)$ [36], where the four-lobe pattern was attributed to the p character of the initial state orbital, that observation was considered as an evidence of the intershell initial state effect. This hypothesis was then proved by calculations. The present results further support this conclusion because the SC3-S model, which employs an independent electron HF wavefunction, does not predict any structure in the region $\theta_{12} < 90^\circ$, while the other two models with a multi-configurational initial state predict two extra lobes in the TDCS, although their relative intensity appears to be different from the

experiment. The source of the extra feature in the region $\theta_{12} < 90^\circ$ is clearly due to the non-Gaussian part of the $|a_{g,u}|^2$ functions (compare figures 3 and 4), where a 'side feature' appears at small relative angles in the Ne case. Another important difference, already highlighted by the study of the equal energy sharing case [15], is clearly visible at $\theta_1 = 30^\circ$ and 60°. The two main lobes appear to be located at smaller relative angle and to have narrower widths in the Ne case. This observation has a correspondence with narrower widths of the Ne $|a_{g,u}|^2$ Gaussian functions with respect to the He ones. The predictions of both CCC and SC3-MC theories are consistent with the experimental data (table 2). The narrower widths of the lobes can be ascribed to a stronger electron correlation in the Ne system. In contrast, no obvious effect is visible on the relative intensity of these two main lobes. So we could state that the present results are qualitatively comparable to the equal energy sharing case.

It is interesting to note that the major differences between the He and Ne cases, as well as between the equal and unequal energy sharing conditions appear at $\theta_1 = 0^\circ$ and particularly for the antiparallel emission. This is also the condition where the largest difference between theory and experiment is observed. Indeed, this is by far the most difficult geometry for theoretical and experimental determinations due to the small value of the cross section (evident from the vertical scale reported in figure 2, the scattering of the data points and their error bars) and the dominance of the ungerade amplitude of the TDCS, which is about two orders of magnitude smaller than the gerade one (see table 2).

In Ne, similarly to He, the ungerade amplitude when parameterized with a Gaussian function is characterized by a narrower width than the gerade one. Furthermore, these two amplitudes maintained a difference in intensities of about two orders of magnitude.

The comparison among the experimental and theoretical amplitudes and phase summarized in table 2 can be used to achieve a better understanding of the differences between experiment and theory as well as among the different theoretical models. In the He case, the SC3 model predicts (i) larger $\Gamma'_{g,u}s$ that result in lobes slightly shifted with respect to the experimental ones at $\theta_1 = 30^\circ$ and 60° and, more important, (ii) a too small A_g/A_u ratio which is mainly responsible for the too large intensity of the lobes in the backward plane. In the case of Ne, the main difference between the experiment and CCC and SC3-MC is in the A_g/A_u ratio. In both models, the ratio is overestimated. This results in a low relative intensity for the kinematics with $\theta_1 = 0^\circ$ around $\theta_{12} = 180^\circ$ as compared to the lobes at $\theta_{12} = 120^\circ$ and 240°.

The other difference between the two models is the behaviour of $\cos\delta$ with θ_{12}. In the case of He, both models agree between themselves and with the experimental value in the θ_{12} region investigated by the experiment. Then they predict phases with opposite sign in the region $\theta_{12} < 110^\circ$ where no experimental data are available. In the case of Ne, only the CCC prediction is consistent with the experiment at $\theta_{12} \geqslant 150^\circ$. The value of the relative phase between the two amplitudes determines the interference term in the TDCS. This affects mainly the relative intensities of the different features in the TDCS (for example, a constant and positive $\cos\delta$ reduces and may even completely cancel out the backward lobe at $\theta_2 = 180^\circ$ in the TDCS measured with $\theta_1 = 0^\circ$) and shifts slightly the position and widths of the lobes.

6. Conclusions

The TDCSs of the $He^{2+}(1s^{-2})$ and $Ne^{2+}(2s^{-2})$ states have been measured at the same excess energy with respect to their relative threshold under unequal energy sharing conditions. As already found in an analogous study under equal energy sharing conditions [14], despite that the two cases share the same initial and final state symmetries some qualitative differences are

observed in the TDCS. However, at variance with the equal energy sharing case the differences cannot be explained only as an initial state effect. Indeed, the comparison with two different models which use an accurate Ne 2s initial state wavefunction, which accounts for 2s–2p intrashell correlation, still displays some disagreement. This finding suggests that a complete description of the observed TDCS implies an extension of the used models to account properly for the correlation between the ejected electrons and the bound ones in the final state.

The comparison of the experimental results with the theoretical predictions of both analytical (SC3) and computational (CCC) theories has shown that both methods now have the capability of making reliable predictions of the shape of the TDCS for atomic systems heavier than He, provided an accurate initial state wavefunction is used.

The method proposed by Bolognesi *et al* [5] is used for extracting the basic dynamical parameters of the TDCS, i.e. the square modulus of the gerade and ungerade amplitudes and the cosine function of their relative phase δ. When applied to both experimental and theoretical data, this method again proved to be very useful for identifying the source of discrepancy between experiment and theory as well as between different theoretical models. This is the first time that information on the ungerade amplitude for an atomic system other than He is obtained.

Then, the combination of a set of internormalized data together with the previous data has allowed us to investigate the differences in the predictions of the absolute value of the TDCS.

It would be interesting to extend this kind of joint experimental and theoretical study to other challenging situations as the measurement of the TDCS using circularly polarized light, which will also provide the sign of the phase or the measurement of the PDI of the ns^2 ($n > 2$) states of the other rare gases. These TDCSs have been recently measured under equal energy sharing [37] conditions. The results show an interesting and systematic evolution of the forward lobes at $\theta_1 = 0^\circ$ as the size of the atom is increased which is waiting for theoretical interpretation.

Acknowledgments

This work was partially supported by the MIUR FIRB project 'Probing the microscopic dynamics of chemical reactivity'. VF thanks the ICTP for a TRIL scholarship. AK thanks the CNR—Short Term Mobility Program for supporting his visit to CNR-IMIP and Synchrotron Elettra (Trieste). Work in Argentina has been supported by grant PICTR 03/00437 of the ANPCYT.

References

[1] Schwarzkopf O, Krässig B, Elmiger J and Schmidt V 1993 *Phys. Rev. Lett.* **70** 3008
[2] Ullrich J, Moshammer R, Dörner R, Jagutzki O, Mergel V, Schmidt-Böcking H and Spielberger L 1997 *J. Phys. B: At. Mol. Opt. Phys.* **30** 2917
[3] Huetz A and Avaldi L 2005 *J. Phys. B: At. Mol. Opt. Phys.* **38** S861
Bolognesi P, King G C and Avaldi L 2004 *Radiat. Phys. Chem.* **70** 207
Avaldi L and King G C 2000 *J. Phys. B: At. Mol. Opt. Phys.* **33** R215
[4] Briggs J S and Schmidt V 2000 *J. Phys. B: At. Mol. Opt. Phys.* **33** R1
[5] Bolognesi P, Kheifets A S, Bray I, Malegat L, Selles P, Kazansky A K and Avaldi L 2003 *J. Phys. B: At. Mol. Opt. Phys.* **36** L241
[6] Krässig B 2001 Correlations, polarization and ionization in atomic systems *AIP Conf. Proc. (Rolla, USA)* vol 604 ed D H Madison and M Schulz p 12
Knapp A *et al* 2005 *J. Phys. B: At. Mol. Opt. Phys.* **38** 645
[7] Bolognesi P, Zitnik M, Malegat L, Selles P, Turri G, Coreno M, Camilloni R and Avaldi L 2004 *J. Phys. B: At. Mol. Opt. Phys.* **37** 2285

[8] Kazansky A K and Ostrovsky V N 1995 *Phys. Rev.* A **51** 3712
Kazansky A K and Ostrovsky V N 1995 *J. Phys. B: At. Mol. Opt. Phys.* **28** L333
Kazansky A K and Ostrovsky V N 1995 *Phys. Rev.* A **52** 1775
[9] Maulbetsch F and Briggs J J 1995 *J. Phys. B: At. Mol. Opt. Phys.* **28** 551
[10] Malcherek A W, Maulbetsch F and Briggs J S 1996 *J. Phys. B: At. Mol. Opt. Phys.* **29** 4127
[11] Schaphorst S J, Krässig B, Schwarzkopf O, Scherer N and Schmidt V 1995 *J. Phys. B: At. Mol. Opt. Phys.* **28** L233
[12] Malegat L, Selles P and Huetz A 1997 *J. Phys. B: At. Mol. Opt. Phys.* **30** 251
[13] Schaphorst S J, Krässig B, Schwarzkopf O, Scherer N, Schmidt V, Lablanquie P, Andric L, Mazeau J and Huetz A 1995 *J. Electron Spectrosc. Relat. Phenom.* **76** 229
[14] Bolognesi P, Flammini R, Kheifets A, Bray I and Avaldi L 2004 *Phys. Rev.* A **70** 062715
[15] Bolognesi P, Otranto S, Garibotti C R, Flammini R, Alberti G and Avaldi L 2005 *J. Electron Spectrosc. Relat. Phenom.* **144–147** 63
[16] Kheifets A and Bray I 1998 *Phys. Rev. Lett.* **81** 4588
Kheifets A and Bray I 1988 *J. Phys. B: At. Mol. Opt. Phys.* **31** L447
[17] Otranto S and Garibotti C R 2002 *Eur. Phys. J.* D **21** 285
[18] Blyth R R *et al* 1999 *J. Electron Spectrosc. Relat. Phenom.* **101–103** 959
[19] Diviacco B, Bracco R, Poloni C, Walke R P and Zangardo D 1992 *Rev. Sci. Instrum.* **63** 388
[20] Melpignano P, Di Fonzo S, Bianco A and Jark W 1995 *Rev. Sci. Instrum.* **66** 2125
[21] Krässig B, Schwarzkopft O and Schmidt V 1993 *J. Phys. B: At. Mol. Opt. Phys.* **26** 2589
[22] Bolognesi P, Coreno M, Alberti G, Richter R, Sankari R and Avaldi L 2004 *J. Electron Spectrosc. Relat. Phenom.* **141** 105
[23] Wehlitz R, Langer B, Berrah N, Whitfield S B, Viefhaus J and Becker U J 1993 *J. Phys. B: At. Mol. Opt. Phys.* **26** L783
[24] Garibotti C R and Miraglia J E 1980 *Phys. Rev.* A **21** 572
[25] Maulbetsch F and Briggs J S 1992 *Phys. Rev. Lett.* **68** 2004
[26] Belkic D, Gayet R and Salin A 1979 *Phys. Rep.* **56** 279
[27] Avaldi L, Dawber G, Gulley N, Rojas H, King G C, Hall R, Stuhec M and Zitnik M 1997 *J. Phys. B: At. Mol. Opt. Phys.* **30** 5197
[28] Schartner K H, Mentzel G, Magel B, Möbus B, Ehresmann A, Vollweiler F and Schmoranzer H J 1993 *J. Phys. B: At. Mol. Opt. Phys.* **26** 445
[29] Persson W, Wahlström C-G and Jönsson L 1991 *Phys. Rev.* A **43** 4791
[30] Koga T, Tatewaki H and Thakkar A J 1993 *Phys. Rev.* A **47** 4510
[31] Bräuning H *et al* 1998 *J. Phys. B: At. Mol. Opt. Phys.* **31** 5149
[32] Collin S A, Huetz A, Reddish T J, Seccombe D P and Soejima K 2001 *Phys. Rev.* A **64** 62706
[33] Huetz A, Selles P, Waymel D and Mazeau J 1991 *J. Phys. B: At. Mol. Opt. Phys.* **24** 1917
[34] Kheifets A and Bray I 2002 *Phys. Rev.* A **65** 022708
[35] Cvejanovic S and Reddish T J 2000 *J. Phys. B: At. Mol. Opt. Phys.* **33** 4691
[36] Schaphorst S J, Krässig B, Schwarzkopf O, Scherer N and Schmidt V 1996 *J. Phys. B: At. Mol. Opt. Phys.* **29** 4225
[37] Bolognesi P *et al* 2004 *Phys. Scr.* T **110** 62